

## Numerical Study of the Moving Boundary Problem During Melting Process in a Rectangular Cavity Heated from Below

Y. Jellouli, R. Chouikh, A. Guizani and A. Belghith  
CRTE/LEPT BP 95 Hammam Lif 2050, Tunisia

---

**Abstract:** We present an analysis of the melting process in Phase Change Materials (PCM) in a horizontal cavity heated from below, driven by the coupling of transient heat conduction in the solid phase and steady state laminar natural convection in the liquid phase with one of the boundaries of the solution domain that moves. We state the problem in the Cartesian coordinate system; involve the use of a control volume method to solve the full vorticity equation together with the stream function and energy equation. The moving boundary was linearized by a coordinate transformation and immobilized in step time calculation. The results show that the melting front was stabilized at a well defined position when the steady state was reached and the higher solid phase was preserved.

**Key words:** Cooling storage, pseudo-convection, interface solid-liquid, modelling

---

### INTRODUCTION

The amount of work accomplished in the area of cooling storage by phase change in a PCM has increased in the last years. There is a growing demand for a better understanding of the phase change kinematics in order to optimize the cycles of storage discharging. In fact, interest in utilising clean energy sources, such as solar energy, is growing because of environmental considerations. However, due to its periodic nature, a thermal energy storage device is needed. Although the majority of the work accomplished in this area has been targeted towards practical applications, limited theoretical modelling has also been done to support the experimental work. Heat transfer in the thermal energy storage systems is a conjugated phase change-convection problem. So, the mathematical complexities are much more involved than the natural heat convection case. The coupling and non-linearity of the governing equations and the complicated geometries involved by the moving boundary have forced experimental solution.

Rieger *et al.*<sup>[1]</sup> established a numerical treatment of the mobile boundary problem for a PCM in melting around horizontal roll. They presented the influence of the natural convection on the melting process with Rayleigh number  $Ra$  going up to  $1.5 \cdot 10^5$ , Stefan number ranging between  $5 \cdot 10^{-3}$  and  $8 \cdot 10^{-3}$  and Prandtl number  $Pr = 50$ .

In the same way, Prud'homme *et al.*<sup>[2]</sup> studied the melting inside a cylindrical PCM configuration heated by bottom, but without taking account of the effect of the heat transfer by conduction in the solid phase in the calculation of the heat transfer through the solid-liquid interface. The mathematical model used consists in solving the coupled of Naviers-Stokes equations and the energy balance equation at the interface.

Hsu *et al.*<sup>[3]</sup> dealt with the numerical study, the problem of the mobile border in the case of a heated cylinder drowned in a PCM by the control volume

method. The discretization of the equations required the immobilization of the border for one length of time  $\Delta t$  well defined. For this length of time, the mass of the solid phase melted seems to pass through the surface delimiting the control volume. From this surface one then defines what is called the pseudo-convection which has a very significant role on the dynamics of the thermal transfer.

Bénard *et al.*<sup>[4]</sup> resumed the work of Hsu *et al.*<sup>[3]</sup> for the same cylindrical geometry and studied the influence of conduction on the speed of the melting process. They specified the assumptions which help evaluating the order of magnitude of each phenomenon: the convective flow is not influenced by the movement of the interface, the natural convection is stationary with each step of time and the melting process is assimilated like a succession of steps of quasi-stationary time.

Fteiti *et al.*<sup>[5]</sup> studied the melting process of a PCM in a square enclosure heated from below, cooled from the top and the remaining walls are insulated. They presented a numerical simulation where the heat transfer equations were expressed on all the domain of the MCP. The quantities of liquid and solid were defined thanks to the liquid fraction coefficient. They concluded that the melting process is more rapid as the aspect ratio is small, but the volume fraction melted at the steady state is less important.

In conclusion, let us note that fusion by bottom in a confined space is a problem which requires even more attention. The complexity of this problem comes from the problem of the development of the thermo-convective instabilities of Rayleigh-Bénard, coupled with a moving border and a zone of variable flow thickness.

This work aims to deepen the understanding of heat transfer mechanisms happening during the moving boundary problem in a melting process controlled by natural convection in the liquid and conduction in the solid. The study is based upon numerical solutions of energy and Navier-Stokes equations in the liquid phase

and energy equation in the solid phase together with energy balance equation in the solid-liquid interface. We used a control volume method which separates the liquid and the solid domain.

**Physical problem and governing equations:** Figure 1 presents a schematic drawing of a vertical cross section of the rectangular H x L enclosure containing the PCM. The depth of the enclosure is presumed to be long enough so that the end walls in the y direction do not affect the behaviour significantly. Hence, the process may be considered as two dimensional in the x,z plane.

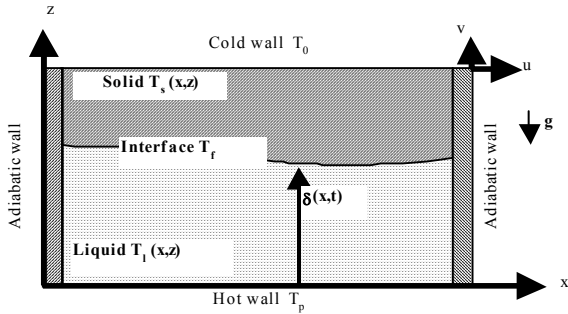


Fig. 1: Configuration geometric

The equations which describe this problem are those expressing the conservation of mass, momentum and energy. The main assumptions made concern the liquid which is considered an incompressible Newtonian fluid and the physical properties of this fluid are constant except for density variations which affect the buoyancy. Also, the thermo-physical properties are constant for the temperature range considered in both phases.

The complete set of equation to be solved in the dimensional form is then:

**\*Liquid phase**

$$\frac{\partial^2 \psi}{\partial x^2} + \frac{\partial^2 \psi}{\partial z^2} = -\omega \quad (1)$$

$$u \frac{\partial(\omega)}{\partial x} + v \frac{\partial(\omega)}{\partial z} = \nu_l \left[ \frac{\partial^2 \omega}{\partial x^2} + \frac{\partial^2 \omega}{\partial z^2} \right] + \beta g \frac{\partial T_l}{\partial x} \quad (2)$$

$$u \frac{\partial(T_l)}{\partial x} + v \frac{\partial(T_l)}{\partial z} = \alpha_l \left[ \frac{\partial^2 T_l}{\partial x^2} + \frac{\partial^2 T_l}{\partial z^2} \right] \quad (3)$$

**\*Solid phase**

$$\frac{\partial T_s}{\partial t} = \alpha_s \left[ \frac{\partial^2 T_s}{\partial x^2} + \frac{\partial^2 T_s}{\partial z^2} \right] \quad (4)$$

**\*Solid-liquid interface**

$$\left[ 1 + \left( \frac{\partial \delta}{\partial x} \right)^2 \right] \left( \lambda_s \frac{\partial T_s}{\partial z} \right)_{z=\delta(x,t)} - \left[ 1 + \left( \frac{\partial \delta}{\partial x} \right)^2 \right] \left( \lambda_l \frac{\partial T_l}{\partial z} \right)_{z=\delta(x,t)} = \rho_s L_f \frac{\partial \delta}{\partial t} \quad (5)$$

The right hand side of this equation represents the energy absorbed by the conversion of solid into liquid. On the left hand side, the first term represents the heat conducted into the solid from the interface and the second term expresses the heat delivered to the interface from the liquid by conduction.

The coordinates transformation and the dimensionless coordinates chosen are given below:

**\*Liquid phase**

$$X_l = x^* \text{ and } Z_l = \frac{z^*}{\Delta}$$

**\*Solid phase**

$$X_s = x^* \text{ and } Z_s = \frac{A^{-1} - z^*}{1 - \Delta}$$

The governing equations of the melting process are then in the dimensionless form as follows:

**\* Liquid phase**

$$\frac{\partial^2 \psi^*}{\partial X_l^{*2}} + \frac{1}{\Delta^2} \frac{\partial^2 \psi^*}{\partial Z_l^{*2}} = -\omega^* \quad (6)$$

$$\frac{\partial(u^* \omega^*)}{\partial X_l} + \frac{1}{\Delta} \frac{\partial(v^* \omega^*)}{\partial Z_l} \quad (7)$$

$$= -\frac{\text{Pr}}{\text{Ra}^{3/4}} \left( \frac{\partial^2 \omega^*}{\partial X_l} + \frac{1}{\Delta^2} \frac{\partial^2 \omega^*}{\partial Z_l} \right) + \text{Ra Pr} \frac{\partial \theta_l}{\partial X_l}$$

$$\frac{\partial(u^* \theta_l)}{\partial X_l} + \frac{1}{\Delta} \frac{\partial(v^* \theta_l)}{\partial Z_l} = -\frac{1}{\text{Ra}^{3/4}} \left( \frac{\partial^2 \theta_l}{\partial X_l} + \frac{1}{\Delta^2} \frac{\partial^2 \theta_l}{\partial Z_l} \right) \quad (8)$$

**\* Solid phase**

$$\frac{\partial \theta_s}{\partial t^*} = \frac{\alpha^*}{\text{Pr Ra}} \left\{ \frac{\partial^2 \theta_s}{\partial X_s^2} + \left[ \left( \frac{Z_s}{1-\Delta} \right)^2 + \left( \frac{\partial \Delta}{\partial X_s} \right)^2 \right] \frac{\partial^2 \theta_s}{\partial Z_s^2} - 2 \frac{Z_s}{1-\Delta} \frac{\partial \Delta}{\partial X_s} \frac{\partial \theta_s}{\partial X_s} \frac{\partial \theta_s}{\partial Z_s} \right\} \quad (9)$$

$$+ \frac{Z_s}{1-\Delta} \frac{\partial \Delta}{\partial t^*} \frac{\partial \theta_s}{\partial Z_s}$$

**\* Solid-liquid interface**

$$\left[ 1 + \left( \frac{\partial \delta^*}{\partial X_l} \right)^2 \right] \left[ \lambda^* \Delta T \left( -\frac{1}{1-\Delta} \right) \left( \frac{\partial \theta_s}{\partial Z_s} \right)_{Z_s=A^{-1}} - \frac{1}{\Delta} \left( \frac{\partial \theta_l}{\partial Z_l} \right)_{Z_l=A^{-1}} \right] \quad (10)$$

$$= \frac{\text{Pr Ra}}{\text{Ste}^*} \frac{\partial \delta^*}{\partial t^*}$$

As indicated in<sup>[4]</sup>, we define the pseudo liquid Nusselt number  $Nu_L$  and the pseudo solid Nusselt number  $Nu_S$  at the interface by:

$$Nu_s = \left[ 1 + \left( \frac{\partial \delta^*}{\partial X_l} \right)^2 \right] \left( -\frac{1}{1-\Delta} \right) \left( \frac{\partial \theta_s}{\partial Z_s} \right)_{Z_s=A-l} \quad (11)$$

and  $Nu_l = \left[ 1 + \left( \frac{\partial \delta^*}{\partial X_l} \right)^2 \right] \frac{1}{\Delta} \left( \frac{\partial \theta_l}{\partial Z_l} \right)_{Z_l=A-l}$

These equations are solved by taking account of the walls adherence condition and of the adiabatic vertical walls for the two phases.

**Solution procedure:** The transient heat conduction equation in the solid domain and the coupled elliptic transport equations for  $\omega^*$ ,  $\psi^*$  and  $T^*$  are solved numerically using the control volume scheme developed by Patankar<sup>[6]</sup>. The set of linear equations is solved by using the Simultaneous Over-Relaxation method (S.O.R) coupled with the Chebychev algorithm. The solution was considered converged when the relative error of the considered variable becomes less than  $10^{-4}$ . The method employed has been successfully used for solving complex problems like this<sup>[7]</sup>. Finally, we use in the present study unequally spaced grids that provide good results with a minimum number of computational points. Indeed, after a series of test runs, the number of the grid points is fixed at 20 x 30 in the liquid phase and 10 x 30 in the solid phase for all cases. The numerical procedure is started with a pure one-dimensional conduction model in the solid domain and is terminated when the required time for the onset of convection in the melt layer is reached<sup>[4]</sup>. Then, a first resolution of the coupled equations of  $\omega^*$ ,  $\psi^*$  and  $T^*$  is done in the initial rectangular cavity. Furthermore, the numerical approach used an iterative procedure to solve the coupled heat conduction equation in the solid domain and interface equation. In fact, the temperature distribution in the solid phase is needed to solve the energy equation which defines the movement of the interface. We note that the fusion time is the time step during which natural convection heat transfer at the interface is considered to be constant. This fusion step is divided into a number of conduction steps which can be taken small to ensure a good precision of the calculation of the temperature field in the solid phase. This iterative procedure is repeated at each conduction step and a new grid is generated in both phases. At the end of a fusion step, a new position of the liquid-solid interface is obtained as well as the time dependent temperature distribution in the solid phase. The natural convection problem in the newly defined liquid cavity is solved again. This numerical procedure is repeated until the stationary position of the interface is reached.

**RESULTS AND DISCUSSION**

The melting process begins at time  $t=0$ , when the bottom side temperature of the cavity is raised to a

constant temperature above the fusion temperature of the PCM. The dimensionless numbers considered in this study are :  $Pr = 54$ ,  $Ra = 10^6$  and  $Ste = 6,94 \cdot 10^{-2}$ . In order to give an idea about the shape of the interface during the evolution process, isotherms are discussed first, followed by some representative temperature profile and finally the calculated heat transfer results are presented.

The simulated time evolution of the temperature fields in both phases is illustrated on the isotherms plotted in Fig. 2. In each of the graphs, the isotherm labelled with zero represents the liquid-solid interface during the melting from below in the rectangular closed enclosure filled initially with the PCM in the solid state which represents the element of storage.

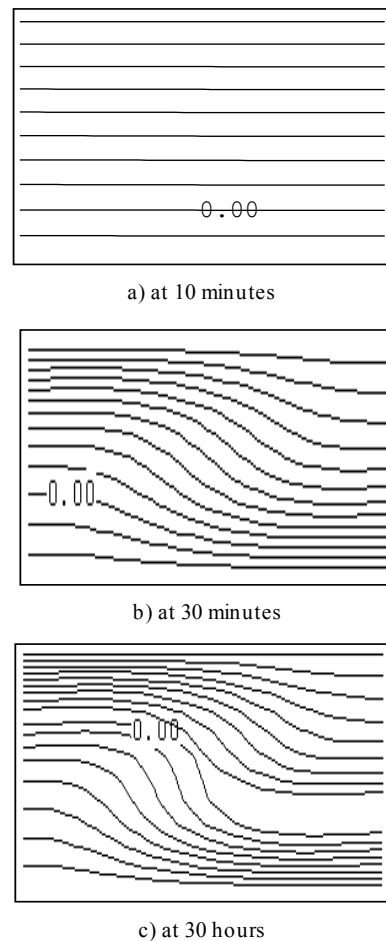


Fig. 2: Isotherms in the whole domain

As can be seen, at the beginning of the melting process, a dominating role of heat conduction can be deduced. In fact, the isotherms are parallel to the hot bottom side of the enclosure. During this early stage, buoyancy forces cannot overcome the resistance

imposed by viscous forces. The effect of convection is seen as a departure of the isotherms from the horizontal.

As time elapses, the deformation of the isotherms and then the interface liquid-solid, becomes more accentuated and the mechanism of transfer of heat is gradually shifted to natural convection. The fact that the cold fluid is above the warm one leads to the development of the thermo-convective instabilities, which alters this kind of a nearly uniform propagation of the heat.

The zone near the hot bottom side is characterized by steep temperature gradients which initiate and maintain the natural convection flow within the liquid phase and gradually influences the local heat transfer rate and therefore the melting characteristics of the system.

During the melting process, the liquid-solid interface which is flat at early stage becomes more distorted as the fluid motion is intensified in the liquid phase. The non-uniform heat transfer distribution along the interface causes the melting front to move faster in the left part of the enclosure and to move more slowly in the right part. The side of the faster motion of the melting front is not imposed by the physics of the problem but rather induced by the round-off errors generated in the numerical computation. The situation is similar to the case of a cavity fully heated from below where the flow field would consist of a single vortex<sup>[5]</sup>. As the interface moves toward the cold top side of the enclosure, the temperature gradient in the solid phase increases and the melting rate decreases. Finally, the melting front reaches a steady position when the heat transfer from the liquid phase is compensated by the heat transfer to the solid phase. The main trends of the melting process are qualitatively similar to what could be observed in previous works<sup>[4]</sup>. At the beginning of the melting from below, heat conduction acts solely but will be superseded gradually by natural convection. However the shape of the interface varies from one study to another, the mathematical complexities of the melting from below are much more involved than in the melting from the side because of the complex moving boundary condition coupled with the thermo-convective instabilities which have a profound influence on the accuracy of predicting the heat transfer in the Phase Change Material<sup>[5]</sup>. Additionally, when the buoyancy forces dominate the viscous ones, the flow in the liquid phase can become unsteady, turbulent and various complex flow structures like three-dimensional convection may appear during this buoyancy induced flow transition.

All this shows that we are far to have exhausted the study of the melting front below since in the absence of the experiments providing flow visualization, all the proposed results can constitute possible theoretical solution.

Figure 3 presents the vertical temperature distribution in the PCM at the mid-width of the enclosure. We note a weak variation of the temperature near the interface indicating that the heat transfer is induced by the melting front movement. This is confirmed in Fig. 4, by the temperature profile in the solid phase of the PCM at time  $t=30$  hours. The transient response of the solid phase due to the temperature step almost reaches a quasi-steady regime in approximately 30 hours, afterwards the temperature distribution remains linear with the increase of the heat flux being mainly due to the movement of the interface.

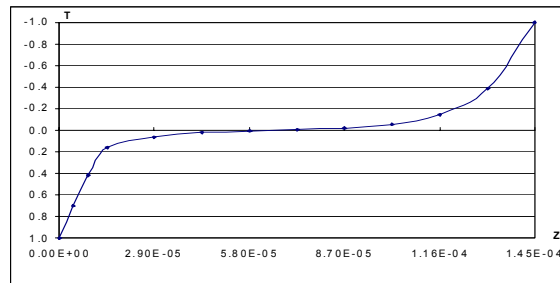


Fig. 3: Temperature profile at the end of the conductive regime

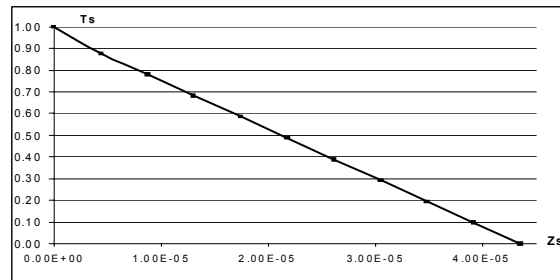


Fig. 4: Temperature profile in the solid at 30 hrs

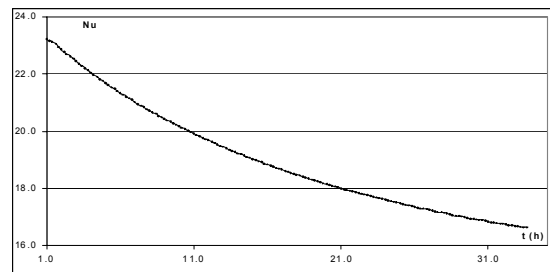


Fig. 5: Average solid Nusselt number

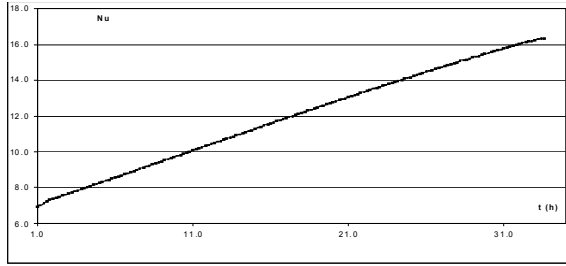


Fig. 6: Average pseudo liquid Nusselt number

Figure 5 and 6 show the time variation of the dimensionless heat flux on both sides of the interface in terms of pseudo Nusselt numbers calculated by the Simpson numerical method.

The average Nusselt number at the interface on the liquid side decreases with time and reaches asymptotically a constant value. Contrarily to the liquid Nusselt number, the average Nusselt number at the interface on the solid side increases progressively as the thickness of the solid domain decreases and then reach approximately the same constant value. This indicates that the heat conducted from the interface is equal to that delivered by conduction from the liquid when the interface reaches a stationary position. This means that at the end of the melting process, the melting front reaches a steady position when the heat transfer from the liquid phase is compensated by the heat transfer to the solid phase.

### CONCLUSION

Numerical results of the moving boundary problem during melting process driven by natural convection in the liquid and conduction in the solid have been obtained for a rectangular cavity heated from below and using an elliptic procedure and a control volume scheme. The agreement between our results and those of study reported earlier was found to be good. In fact, as the melt layer thickness increases with time, natural convection appears in the liquid phase and the non-uniform heat transfer distribution along the interface which reaches a steady position when the heat transfer from the liquid phase is compensated by the heat transfer to the solid phase. The numerical approach presented here appears to be sufficiently versatile to permit computation of other PCM like salt hydrates which presents interesting thermo physical properties useful in cooling storage.

### Nomenclature

#### Latin's numbers

A ratio of L/H  
 C<sub>p</sub> specific heat [J/(kg.K)]  
 g gravitational field [m/s<sup>2</sup>]

H height of the cavity [m]  
 L length of the cavity [m]  
 L<sub>f</sub> latent heat of fusion [J/kg]  
 T temperature [K]

t\*  $\frac{v_l}{L^2} t$  dimensionless time

u\*, v\*  $\frac{(u, v)L}{\alpha_l R_a^{1/4}}$  dimensionless velocity

x\*, z\*  $\frac{(x, z)}{LR_a^{1/2}}$  dimensionless coordinate

X, Z transformed dimensionless coordinate

#### Greek symbols

λ\* dimensionless conductivity λ<sub>l</sub>/λ<sub>s</sub>

α\*  $\frac{\alpha_s}{\alpha_l}$  dimensionless thermal diffusivity

β thermal expansion coefficient [K<sup>-1</sup>]

δ liquid layer thickness [m]

ν kinematical viscosity [m<sup>2</sup>/s]

θ<sub>l</sub>  $(T_l - T_f)/(T_p - T_f)$

θ<sub>s</sub>  $(T_s - T_f)/(T_f - T_0)$

ρ density [kg/m<sup>3</sup>]

ω vorticity

ψ stream function

ω\*  $\frac{\omega L^2 R_a^{1/4}}{\alpha_l}$  dimensionless vorticity

ψ\*  $\frac{\psi}{\alpha_l R_a^{3/4}}$  dimensionless stream function

Δ A δ\*

#### Dimensionless numbers

Pr Prandtl number α<sub>l</sub>/ν<sub>l</sub>

Ra Rayleigh number βgL<sup>3</sup>(T<sub>p</sub>-T<sub>f</sub>)/(α<sub>l</sub>ν<sub>l</sub>)

Ste C<sub>pl</sub>(T<sub>p</sub>-T<sub>f</sub>)/L<sub>f</sub>

Ste\* dimensionless Stefan number Ste/ρ\*

ΔT (T<sub>f</sub>-T<sub>0</sub>)/(T<sub>p</sub>-T<sub>f</sub>)

#### Subscripts

l liquid phase

s solid phase

p bottom wall

0 top wall

c natural convection

f fusion

\* dimensionless variable

### REFERENCES

- Rieger, H., U. Projahn and H. Beer, 1982. Analysis of the heat transport mechanism during melting around a horizontal circular cylinder. Intl. J. Heat Mass Transfer., 25: 137-147.

2. Prud'Homme, M., T. Hung Nguyen and Y.K. Wu, 1991. Simulation numérique de la fusion à l'intérieur d'un cylindre adiabatique chauffé par le bas. *Intl. J. Heat Mass Transfer.*, 34: 2275-2286.
3. Hsu, C.F., E.M. Sparrow and S.V. Patankar, 1981. Numerical solution of moving boundary problems by boundary immobilisation and a control-volume-based finite-difference scheme. *Intl. J. Heat Mass Transfer.*, 24: 1335-1343.
4. Benard, C., D. Gobin and A. Zanolli, 1986. moving boundary problem : heat conduction in the solid phase of phase-change materiel during melting driven by natural convection in the liquid. *Intl. J. Heat Mass Transfer.*, 29: 1669-1681.
5. Fteïti, M. and S. Ben Nasrallah, 2005. Numerical study of interaction between the fluid structure and the moving interface during the melting from below in a rectangular closed enclosure. *Computational Mechanics* 35: 161-169.
6. Patankar, S.V., 1980. *Numerical Heat Transfer and Fluid Flow*. Hemisphere Publishing Corporation.
7. Ben Snoussi, L., R. Chouikh and A. Guizani, 2005. Numerical study of the natural convection flow resulting from the combined buoyancy effects of thermal and mass diffusion in a cavity with differentially heated side walls. *Desalination*, 182: 143-150.